

Chapter 5

A Novel Approach to the Presentation of $p\epsilon$ /pH-Diagrams

M. Kölling, M. Ebert & H.D. Schulz

5.1 Introduction

Classical $p\epsilon$ /pH-diagrams have been constructed assuming an equilibrium between pairs of coexisting species. These conditions yield equations for straight lines where both species show equal activity, separating the $p\epsilon$ /pH-diagram into fields in which one or the other species predominates. These diagrams are usually constructed for systems of low complexity, e.g. an aqueous system with fixed element compositions, at fixed pressure and temperature. Usually, both solid phases and dissolved species are presented in one diagram, in which the stability fields for one or more solid phases are shown.

This simplified diagram conceals some important information which is contained in the underlying calculations for its construction. Although we might be interested to learn which aquatic species are predominant in a solution under conditions at which thermodynamics favours the formation of certain minerals, we do not perceive the distribution of dissolved species in this region. The diagram in Figure 5.1 predicts that magnetite is not stable at $pH = 7$ and $p\epsilon = 10$. Yet, in a

superficial neutral oxid environment magnetite will usually not transform to hematite as it possesses long-term stability.

5.2 Construction of $p\epsilon$ /pH-Diagrams

We are able to construct diagrams as shown in Figure 5.1 using the appropriate NERNST equations of redox reactions related to the mineral of interest. The diagram in Figure 5.1 actually is composed of two diagrams showing the stability of magnetite and hematite in water, with a total iron activity of 10^{-6} M.

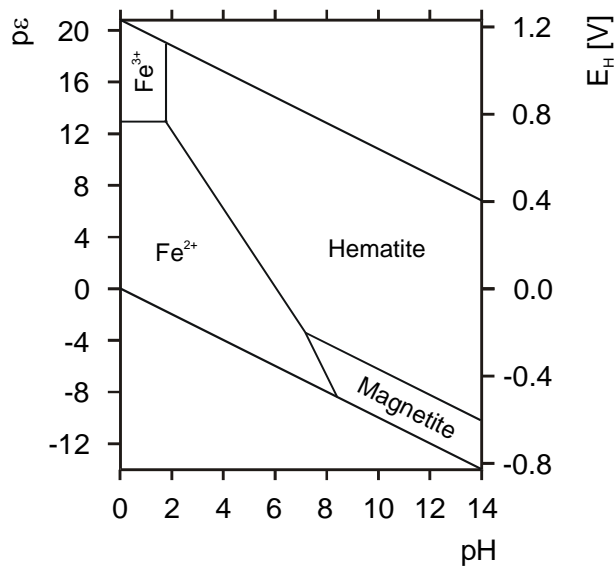
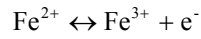


Fig. 5.1: Classical $p\epsilon$ /pH composite diagram after GARRELS & CHRIST (1965) showing the stability fields of hematite and magnetite in water. In areas where none of the considered minerals are stable, the fields of dominant dissolved species are shown. The total activity of dissolved iron is 10^{-6} M.

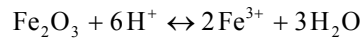
One species distribution visible in this diagram is described by the reaction between Fe^{2+} and Fe^{3+} :



$$p\varepsilon = 13 + \log\left(\frac{[\text{Fe}^{3+}]}{[\text{Fe}^{2+}]}\right) \quad (5.1)$$

$$p\varepsilon = 13 \quad \text{for } [\text{Fe}^{2+}] = [\text{Fe}^{3+}]$$

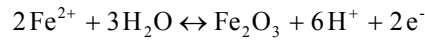
The stability field of hematite is delimited by the reaction with Fe^{3+} :



$$\log[\text{Fe}^{3+}] = -0.72 - 3\text{pH} \quad (5.2)$$

$$\text{pH} = 1.76 \quad \text{for } \log[\text{Fe}^{3+}] = -6$$

and by the reaction with Fe^{2+} :



$$p\varepsilon = 12.34 - \log[\text{Fe}^{2+}] - 3\text{pH} \quad (5.3)$$

$$p\varepsilon = 18.34 - 3\text{pH} \quad \text{for } \log[\text{Fe}^{2+}] = -6$$

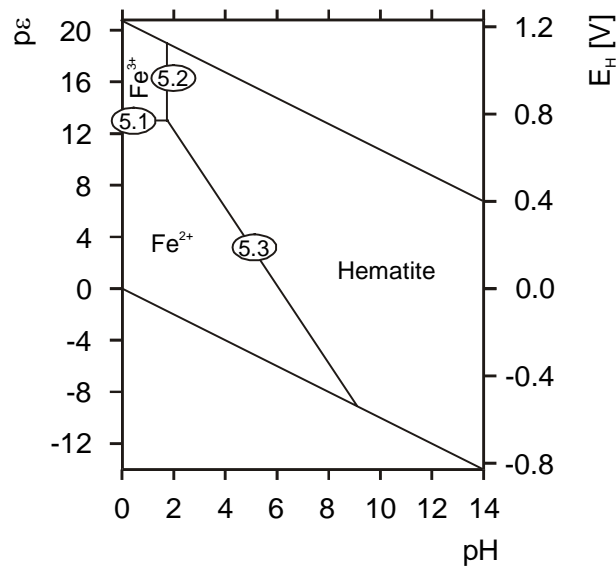
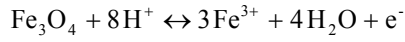


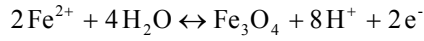
Fig. 5.2: pε/pH-diagram for hematite in water with $\log [\text{Fe}_T] = -6$. Graphical representation of reactions (5.1), (5.2), and (5.3).

Performing the same calculations for magnetite in water we get:



$$p\varepsilon = 5.71 + 3\log[\text{Fe}^{3+}] + 8\text{pH} \quad (5.4)$$

$$p\varepsilon = -12.29 + 8\text{pH} \quad \text{for } \log[\text{Fe}^{3+}] = -6$$



$$p\varepsilon = 16.61 - 1.5\log[\text{Fe}^{2+}] - 4\text{pH} \quad (5.5)$$

$$p\varepsilon = 25.61 - 4\text{pH} \quad \text{for } \log[\text{Fe}^{2+}] = -6$$

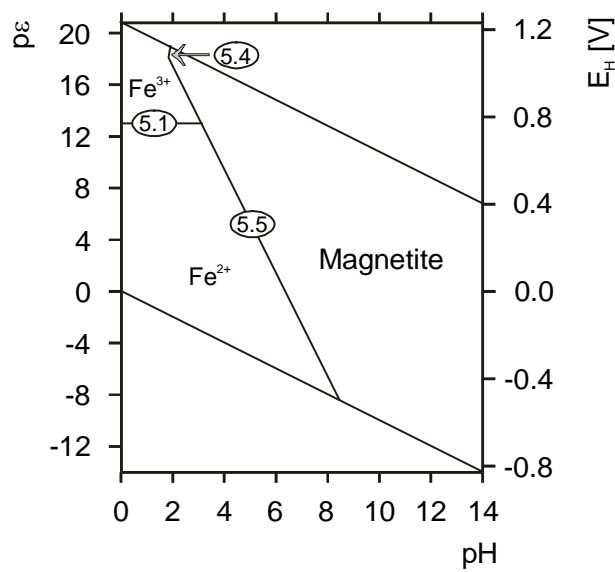


Fig. 5.3: $p\varepsilon/\text{pH}$ -diagram for magnetite in water with $\log [\text{Fe}_T] = -6$. Graphical representation of reactions (5.1), (5.4) and (5.5).

Superimposing Figures 5.2 and 5.3 we get the composite diagram in Figure 5.4. The delimiting line between magnetite and hematite in Figure 5.1 is equal to line (5.6) in this diagram following

$$p\varepsilon = 3.8 - \text{pH} \quad (5.6)$$

It should be noted that opposed to the classical diagram from GARRELS & CHRIST (1965) there are four fields of mineral stability. There are two fields in

which both hematite and magnetite are stable, i.e. both minerals will not be dissolved in water at the given iron activity.

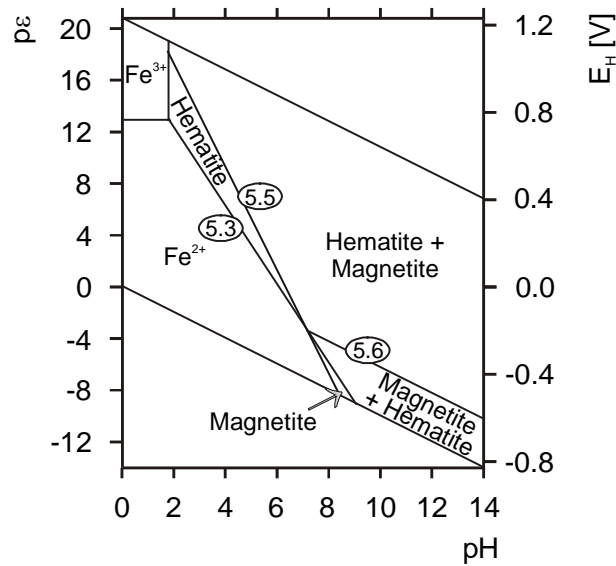


Fig. 5.4: Composite diagram of hematite and magnetite stability in water at $\log [Fe_T] = -6$. Graphical representation of reactions (5.3), (5.5) and (5.6).

In the upper field the water is more supersaturated with respect to hematite and therefore magnetite should thermodynamically be transformed into hematite while in the lower field the magnetite saturation is dominant. There are only small triangular fields in the $p\epsilon/pH$ -diagram in which only hematite or magnetite are stable in water. Therefore, either one of the minerals will be dissolved.

The difference between the diagrams shown in Figures 5.1 and 5.4 is that mineral stability fields of classical diagrams actually demonstrate mineral saturation predominance fields. Yet, in the major parts of the hematite and magnetite fields shown in Figures 5.1, the concurring mineral is stable as well. If we are interested in interactions between water and minerals rather than in re-crystallisation within mineral parageneses, a representation as in Figure 5.4 is a better tool to assess expected reactions in water.

5.3 Disadvantages of Classical $p\epsilon/pH$ -Diagrams

The construction of $p\epsilon/pH$ -diagrams for more complex systems is cumbersome. Usually calculations are performed for pure four- or five-component systems. Therefore such diagrams often are poor approximations to the system of interest.

The construction of straight lines from the condition of equality between two species is illicit. Especially in regions where two lines meet, highest activity of a species may not be correctly calculated from species pairs, since all possible species have to be taken into account. Therefore, within the stability field of one species, the condition "activity of species A > activity of species B" has to be replaced by "activity of species A > activity of all other species". In a three-dimensional $p\epsilon/pH$ -activity-diagram, each species activity is plotted as a bent surface, with the uppermost surface representing the dominant species. The intersecting lines between different surfaces are equivalent to the borders of dominance fields in the classic $p\epsilon/pH$ -diagram. Taking all possible species for every stability field border into account, these borders are no longer strictly straight lines.

$p\epsilon/pH$ -diagrams with rounded predominance field borders have been published (GARRELS & CHRIST, 1965; KRAUSKOPF, 1979). Here, the curved borders result from the fact that the pH dependence of species distributions has been taken into account for carbon and sulfur species. Therefore, more than just pairs of species have been used to construct dominance fields. Three-dimensional diagrams showing the relationships between $p\epsilon/pH$ -and pCO_2 or pS_2 have been published by GARRELS & CHRIST (1965).

Assuming a constant composition in a solution, constant p-T conditions and a selected set of solid phases, part of the $p\epsilon/pH$ -diagram usually shows a stability field for solid phases such that the underlying dominance fields for dissolved species are concealed. In addition, stability fields of solid phases are usually presented as dominance fields where the solid phase with the highest saturation index conceals the underlying stability fields of other solid phases. At the border between two stability fields, the saturation indices of the solid phases are identical.

However, in most natural systems, the phase with the highest saturation index may not be the phase which is actually formed. Other oversaturated phases having a lower saturation index, but a faster rate of precipitation, may form first and control the composition of the solution.

5.4 New Presentation of $p\epsilon/pH$ -Diagrams

To circumvent the disadvantages of classical $p\epsilon/pH$ -diagrams, we would like to suggest a different method of presentation in which a pair of $p\epsilon/pH$ -diagrams is shown, one for the dissolved species and one for the solid phases (Figure 5.5). In one diagram, the dominance fields of dissolved species even is shown in regions where the solid phases are oversaturated.

In the second diagram, overlapping fields are plotted of saturation index $SI > 0$ for the different minerals. As a result, the stability fields of all solid phases are shown rather than just the field belonging to the phase with the highest saturation index.

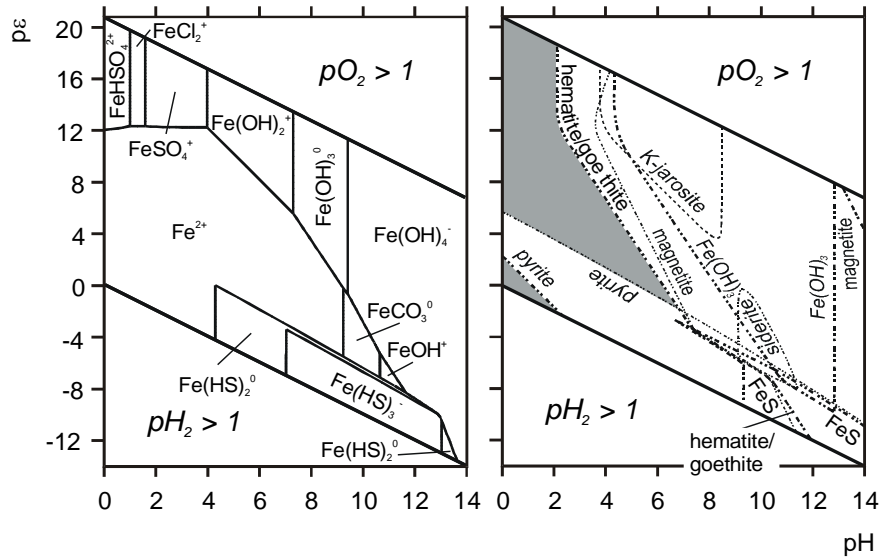


Fig. 5.5: Example for a pair of $p\epsilon/pH$ -diagrams for $3 \mu\text{mol/L}$ Fe in a standard seawater background. *Left:* dominance fields of dissolved iron species. *Right:* overlapping stability fields of different iron minerals. In the shaded area none of the minerals considered are stable. In the classical way of presentation, the dominance fields of the dissolved species are shown only in this area. Note the smooth borders of the stability fields which result from exact calculation of the stability fields accounting for the complete water composition.

To include a greater amount of dissolved species and solid phases, we have performed a series of calculations across the $p\epsilon/pH$ -field using thermodynamic model programs such as PHREEQE (PARKHURST et al. 1980, 1990) and PHREEQC (PARKHURST, 1995). Using a pre-processor for the generation of input files and a post-processor for the extraction of activities and saturation indices under different $p\epsilon/pH$ -conditions, we were able to construct very precise $p\epsilon/pH$ -diagram doublets for both the solid phase stability fields and the dissolved species dominance fields for every system that might be defined in PHREEQE.

Using automated calculation series at a sufficient $p\epsilon/pH$ -resolution some interesting curvatures in the stability fields were revealed. Using this method, $p\epsilon/pH$ -diagrams may be constructed for real waters rather than for four- or five-component-systems.

EBERT et al. (1997) used this mode of presentation to assess chromate transport in an anoxic FeS-quartz-sand system. In Figure 5.6 a pe/pH -diagram doublet for this system is shown. In the species diagram, iron, sulfur and chromium species distributions are superimposed. It should be noted that the diagram includes the pH-range between pH = 6 and pH = 13. In the mineral stability diagram, overlapping fields of mineral saturation are plotted. In the pH-range considered, the diagram area is completely covered with mineral stability fields in such a manner, that in a classical diagram, no information on species distribution is given.

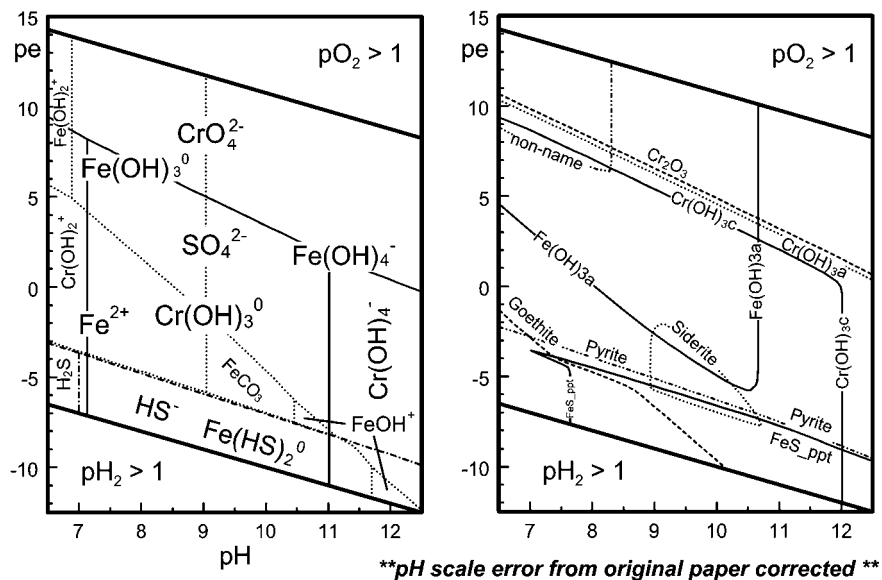


Fig. 5.6: pe/pH -diagram doublet for the assessment of chromate reduction and retention in a slightly alkaline anoxic groundwater system containing FeS (EBERT et al., 1997). The calculations were performed using PHREEQE for Cr (0.5 mM), Fe (1 μ M) and S (0.5 mM) in a real water with Ca (0.26 mM), Mg (0.15 mM), Na (1.9 mM), K (0.1 mM), Mn (3 μ M), Cl (0.63 mM), N (0.4 mM), P (3.1 μ M), and IC (0.92 mM). The data scheme is 4 points per pe and 4 points per pH i.e. this diagram contains data from approximately 2000 PHREEQE runs. Methane formation was neglected. The mineral „no name“ is the jarosite-type $KFe_3(CrO_4)_2(OH)_6$.

The diagrams show that chromate does not coexist with dissolved sulfide or ferrous iron species, nor with the sulfide minerals or the ferrous iron minerals under study. Although the reactions with sulfides should be thermodynamically favoured due to these diagrams, chromate reduction by sulfide only occurs at high chromate levels that inhibit iron reducing bacteria.

5.5 Conclusions

Upon investigating dissolution/precipitation reactions, the composition of the solution in contact with a mineral which, due to oversaturation, is likely to form is of major interest. Using two separate diagrams, one for dissolved species and one for solid phases, opens the view into the regions that are concealed by mineral stability fields in classical diagrams.

Having to assess, whether or not a natural water is aggressive to the mineral of interest, or whether the formation of a certain mineral is thermodynamically possible, although it might not represent the thermodynamically stable phase in the long term, plotting overlapping fields of mineral stability is much more useful than classical plotting of mineral predominance fields.

By applying several series of PHREEQE calculations to any particular pe/pH-range, very precise diagram doublets can be constructed even applied to complex real systems

5.6 References

- EBERT, M.; ISENBECK-SCHRÖTER, M. & KÖLLING, M. (1997): Reduction and retention of chromate in an anoxic quartz-sand-FeS-system – A laboratory study in water-saturated columns.- In: EBERT, M.(1997): Der Einfluß des Redox-Milieus auf die Mobilität von Chrom im durchströmten Aquifer.- Ber. FB Geowiss. Univ. Bremen 101: 70–99.
- GARRELS, R.M. & CHRIST, C.L. (1965): Solutions, Minerals, and Equilibria.- Harper & Row, New York, 450p.
- KRAUSKOPF, K.B.(1979): Introduction to Geochemistry.- 2nd ed. McGraw Hill, New York; 617p.
- PARKHURST, D.L.; THORSTENSON, D.C. & PLUMMER, L.N. (1980): PHREEQE - A Computer Program for Geochemical Calculations. - U.S. Geol. Survey Water Resources Investigations Reports 80-96, Washington D.C.: 210p.
- PARKHURST, D.L.; THORSTENSON, D.C. & PLUMMER, L.N. (1990): PHREEQE - A Computer Program for Geochemical Calculations. (Conversion and Upgrade of the Prime Version of PHREEQE to IBM PC-Compatible Systems by J.V. Tirisanni & P.D. Glynn).- U.S. Geol. Survey Water Resources Investigations Reports 80-96, Washington D.C.: 195p.
- PARKHURST, D.L. (1995): Users guide to PHREEQC: A computer model for speciation, reaction-path, advective-transport, and inverse geochemical calculations.- U.S.Geol.Survey Water Resources Investigations Reports 95-4227, 143p.